Biophysical Chemistry 22 (1985) 107–113
Elsevier

BPC 00930

ELECTRON PARAMAGNETIC RESONANCE AND OPTICAL SPECTROSCOPIC STUDY OF THE Cu^{2+}-tRNA SYSTEM

S. CANNISTRARO, G. GIUGLIARELLI, G. ONORI and E. RONGONI

Gruppo di Biofisica Molecolare, Dipartimento di Fisica dell'Università, I-06100 Perugia, Italy.

Received 9th January 1985
Revised manuscript received 11th April 1985
Accepted 12th April 1985

Key words: EPR; Optical absorption; tRNA; Cu^{2+}

The interaction of copper ions with tRNA has been studied by optical and EPR spectroscopies. The interaction results in two different paramagnetic complexes characterized by a tetragonal symmetry of the ligand electric field sensed by the ions. The complete set of the spin Hamiltonian parameters has been extracted by computer simulation with the Monte Carlo method. Hypotheses concerning the putative ligands are put forward.

Introduction

Transfer ribonucleic acids are small macromolecules (about 25 kDa), made up of 70–80 nucleotides, which play a central role in the biosynthesis process of proteins and in its regulation. Like other nucleic acids, tRNA molecules are polyelectrolytes characterized by a high charge density (one negative charge per nucleotide residue), their secondary and tertiary structure being strongly affected by the presence of mono- and divalent ions. Since changes in these structures modulate the biological function of tRNA, many studies have been devoted to its interaction with a number of divalent ions (mainly Mg^{2+}, Mn^{2+}, Co^{2+}) [1]. Mg^{2+} is the naturally occurring divalent metal ion, its role being highly specific even if it can be replaced by Mn^{2+} in some biochemical reactions [2]. These experimental observations have prompted quite a few studies mainly concerned in characterizing the interactions between paramagnetic Mn^{2+} and tRNA [1,3,4].

However, conflicting conclusions have been drawn from the results obtained so far [1]. It should first be noted that most experiments have been performed at low ionic strength ($f < 0.01$). Under these conditions the tRNA molecules display an 'extended' structure which is mainly controlled by the electrostatic repulsion between the negatively charged adjacent residues; this structure appears to be significantly different from the 'native' one [3]. The Scatchard plots obtained in these conditions have been interpreted in terms of two different classes of ion-binding sites present in the tRNA molecules: from 4 to 6 highly specific and cooperative sites per molecule should belong to one class and about 25 weak sites to the other [1].

More recently, the presence of specific sites in tRNA has also been questioned on the grounds of a more accurate analysis of the results that takes the polyelectrolyte behaviour of the biomolecule into account [4,5]. The conclusion stemming from these arguments is that the search for possible specific binding sites should be conducted at higher ionic strength. In fact, when $f > 0.1$, tRNA occurs in the native conformation even in the absence of divalent ions, their addition resulting in the stabilization of the structure without other conformational changes [3,6].

The few studies so far conducted under these

conditions indicate either the presence of only one strong binding site for Mg^{2+} [7,8] or the absence of such a binding site, at least for Mn^{2+} [9]. The presence of specific ion-binding sites in tRNA molecules thus still remains an open problem. Another open question regards the similarity of the binding properties of Mn^{2+} with respect to Mg^{2+}. We have recently shown that some differences between these ions could exist [10]. It seems that full-shell ions such as Mg^{2+} and Ca^{2+} can only form ion-type bonds with phosphate groups, whereas incomplete-shell transition metals such as Mn^{2+}, Co^{2+}, Ni^{2+} and Zn^{2+} are not only engaged in this type of bond with phosphate but also can form coordination complexes with the tRNA bases. Hence, the very assumption that Mg^{2+} and Mn^{2+} interact with tRNA in identical ways could be questioned [10].

The studies on transition metal complexes are also particularly interesting, since the toxicity of some of these metals may result from their binding to nucleic acids. Cu^{2+} is a suitable probe for studying these complexes, its biological relevance having been ascertained and its magnetic and electronic properties allowing the use of several comparative techniques [11]. Given this, we have studied the interaction of Cu^{2+} with tRNA molecules in aqueous solutions at high ionic stregth. Cu^{2+}, which possesses a $3d^9$ electronic configuration, is characterized by optical and magnetic properties that are highly sensitive to the symmetry and strength of the ligand field provided by the macromolecular sites at which it might from a complex [11]. Consequently, optical absorption and EPR spectroscopies could be used to provide reliable information on the physical parameters of the paramagnetic complex formed between Cu^{2+} and tRNA.

2. Materials and methods

In order to remove divalent cations, yeast unfractionated tRNA (Boehringer, Mannheim) was dialysed at 4°C overnight against 4 l of 0.1 M NaCl, 4×10^{-3} M EDTA (disodium salt), pH 6.5, and then against three changes of 0.1 M NaCl, pH 6.5. The samples stored at −20°C until use. As a rule, tRNA optical absorption at 260 nm was 20 for the measurements carried out in the 400–1400 nm range and 2 for the 230–400 nm measurements. The tRNA nucleotide concentration was determined by assuming a molar extinction coefficient equal to 7500 [12]. Spectral changes following the addition of divalent ions to the tRNA solution were measured at 25 ± 2°C with a Shimadzu model 360 spectrophotometer; 3-ml quartz cells, 1 cm long, were used. The absorption changes in the ultraviolet range (230–350 nm) were detected by the following differential method: a zero baseline was obtained by placing 2.5 ml of the same tRNA solution into each of two cells placed in the sample and the reference compartment. Addition of Cu^{2+} was accomplished by adding to the sample small volumes (10 μl as a rule) of concentrated solutions of $CuCl_2$. An equal volume of solvent was added to the reference cell in order to attain a concentration balance. In this way we were able to record spectral modifications with an absorbance sensitivity of 2×10^{-4}. Unbuffered solutions were used throughout to prevent interaction of Cu^{2+} with buffers. The pH of solutions was checked at the beginning and end of each experiment, ranging between 5.5 and 6.5. The amount of Cu^{2+} added to the tRNA solution was expressed as r, the molar ratio of ion concentration to nucleotide concentration. To prepare samples for study by EPR, aqueous samples of Cu^{2+}-tRNA were placed in 4.7 nm inner diameter precision glass tubes open at both ends, frozen in liquid nitrogen and stored. To record the EPR spectrum, the sample was removed from the glass tube by warming the surface just sufficiently to allow the cylindrical sample to be pushed out of the tube. It was then placed in an E-246 Varian dewar filled with liquid nitrogen. Finally, the tail of the dewar was inserted in the resonant cavity of the spectrometer. EPR spectra was recorded by an X-band Varian E-109 spectrometer having a modulation frequency of 100 kHz. To calculate the experimentally observed g factors, a magnetic field calibration was performed with a Magnion Precision NMR Gaussmeter, model G. 502, the microwave frequency being determined by a Marconi 2440 counter. An aqueous solution of 1 mM Cu^{2+}, in the presence of 0.2 M $NaClO_4$ and 0.02 M HCl

was used to check the sensitivity of the spectrometer from sample to sample and to provide a standardization of the sample EPR intensity.

EPR data acquisition was performed on an HP 86A microcomputer, through a home-made interface connected to an IEE-488 bus. To run simulation and best-fit programs, the same microcomputer was switched to an intelligent terminal of the mainframe computer (a Prime 550/1) through an RS-232-C serial interface and an HP terminal emulator.

3. Results and discussion

3.1. Optical absorption measurements

The study of the optical properties of the d-d transitions may provide a useful means of investigating the characteristics of the nucleic acid ligands of a transition metal ion: the splitting of the d subshell operated by the ligand field leads to low-energy light absorption, the number of the bands and their position in the spectrum being dependent on the symmetry and strength of the ligand field. We have recently shown how these circumstances may be used profitably to study the Cu^{2+}-tRNA complex [13]. The $3d^9$ configuration

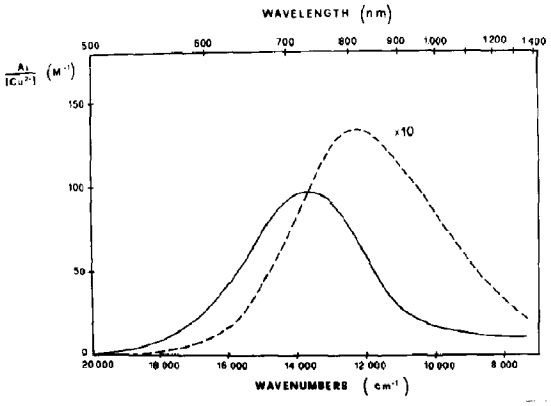

Fig. 1. Optical absorption spectrum of aqueous $[Cu(H_2O)_6]^{2+}$ (— — —) and of the tRNA-Cu^{2+} complex at low r values ($r < 0.08$) (———). The absorption values are divided by the concentration of Cu^{2+} present in solution. Cells with a 1 cm path length were used.

of Cu^{2+} may be considered equivalent to that of a lone electron in the 3d level ($3d^1$). For the free ion, the ground state is five-fold degenerate, the degeneracy being removed according to the symmetry of the crystal ligand field. In the case of octahedral symmetry, the 3d levels are split into two sublevels and only one symmetrical band is expected [14]. If the field possesses tetragonal-bipyramidal symmetry, the 3d level is split into four sublevels and the spectrum should contain three bands. This is the case for Cu^{2+} in water (fig. 1, dashed line) where the ligand field is due to six water dipoles and the observed spectrum has been resolved into the sum of two symmetrical bands with maxima at $\lambda_1 = 790$ and $\lambda_2 = 1060$ nm [14]. In the presence of tRNA molecules at low r values, the spectrum of aqueous Cu^{2+} changes in a characteristic fashion (fig. 1, full line). A marked rise in the absorption (by a factor of about 10), acompanied by a blue shift of the maximum to 730 nm is observed; the band, moreover, turns out to be symmetrical around this maximum and can no longer be resolved into the sum of two component bands as in the case of Cu^{2+} in water.

If we denote the molar extinction coefficient of the copper bound to the tRNA and of the free copper in solution by ϵ_b and ϵ_f, respectively, and the optical path by l, we can write for the absorption spectrum:

$$A_\lambda = [Cu^{2+}]_b \epsilon_b l + [Cu^{2+}]_f \epsilon_f l \qquad (1)$$

If, from this spectrum, we subtract that of a copper solution having a concentration equal to $[Cu^{2+}]_b + [Cu^{2+}]_f$ (or, in other words, all the copper added) we obtained the quantity:

$$\Delta A_\lambda = [Cu^{2+}]_b (\epsilon_b - \epsilon_f) l \qquad (2)$$

which turns out be proportional to the concentration of just the bound copper.

Fig. 2 shows the value of $\Delta A_{730}/A_{260}$ as a function of r; this quantity increases linearly with a sharp break in the linear coefficient at $r \simeq 0.085$ The observed behavior seems to be consistent with the existence of two classes of binding sites: a first class which is occupied up to a value of $r \simeq 0.085$, corresponding to about six Cu^{2+} per molecule of tRNA, and a second one which corresponds to the

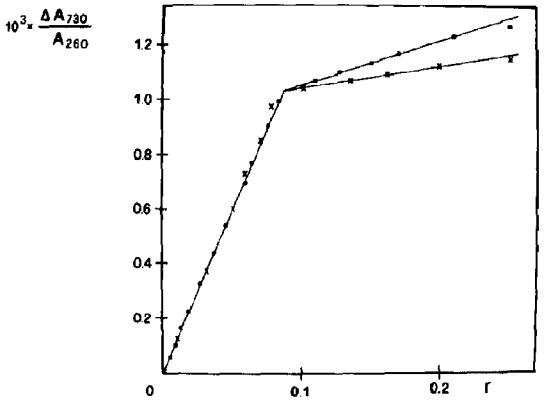

Fig. 2. Differential absorption values, ΔA_{730}, of the tRNA-Cu^{2+} complex and of aqueous $[Cu(H_2O)_6]^{2+}$ at $\lambda = 730$ nm, as a function of r for two different Na^+ concentrations: (●) $[Na^+] = 0.1$ M (×) $[Na^+] = 0.6$ M. ΔA_{730} was normalized with respect to A_{260}.

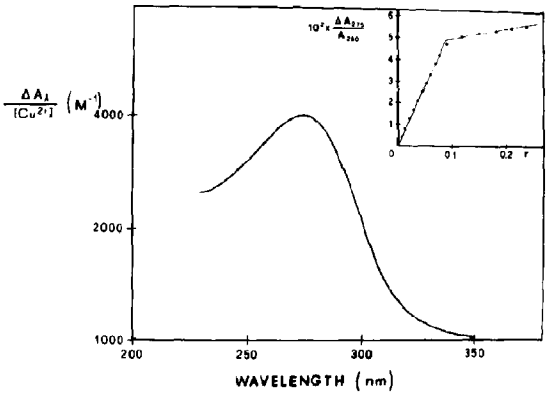

Fig. 3. Ultraviolet difference spectrum for the tRNA-Cu^{2+} complex at low r values. This difference spectrum shows a maximum at about 275 nm whose value, indicated by ΔA_{275}, increases linearly with the copper added. A plot of ΔA_{275} vs. r shows a break at $r \cong 0.085$ (see inset).

formation of a complex having a lower molar extinction coefficient (see eq. 2). As the ionic strength is increased (from 0.1 to 0.6) the formation of the first complex is not significantly modified (low r values) while the formation of the second complex (high r values) is partly inhibited. Similar indications are to be found in a study of the spectral variations in the absorption bands of tRNA in the wavelength range 230–250 nm. Such variations may, in principle, be divided into two groups: charge-transfer transitions which involve both the ligands and the metal ion, and transitions occurring predominantly on the ligands which may be modified by complexation.

If we measure the absorption of a solution of tRNA-Cu^{2+} against a solution of tRNA and of Cu^{2+} separate from the tRNA but of the same concentration, we obtain a characteristic differential spectrum whose amplitude ΔA_λ, for low r values, increases proportionally to the concentration of copper (fig. 3). This differential spectrum indicates the appearence of an absorption band with a maximum at about 275 nm; the high molar absorption ($\sim 4000\ M^{-1}\,cm^{-1}$) suggests the attribution of this band to a charge-transfer transition from a ligand to the metal ion. As r increases, we observe a sharp variation in the shape of the differential spectrum corresponding to $r \simeq 0.085$ (see insert to fig. 3). The variation observed in the differential spectrum at high r values, $\Delta(\Delta A)/\Delta r$, shows a wide maximum between 280 and 290 nm, a minimum at 247 nm and two isobestic points, one at 261 nm and the other at 235 nm (fig. 4). This spectrum is totally analogous to that seen for the DNA-Cu^{2+} complex [15] and could be indicative of a perturbation of the base electronic structure due to a direct binding of metal ions to the bases.

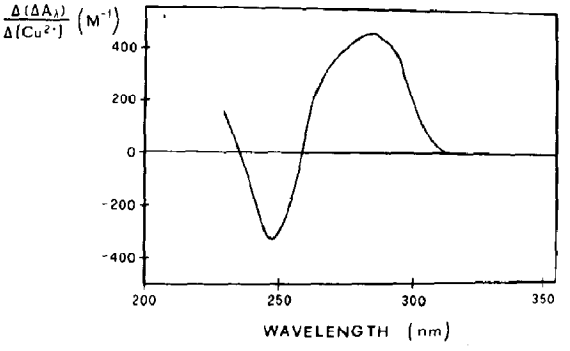

Fig. 4. Plot of the variation observed in the ultraviolet difference spectrum ΔA_λ for the tRNA-Cu^{2+} complex at high r values. The spectrum shown was obtained from the difference between the spectra ΔA_λ (see fig. 3) at $r = 0.15$ ($[Cu^{2+}] = 4 \times 10^{-5}$ M) and $r = 0.12$ ($[Cu^{2+}] = 3.2 \times 10^{-5}$ M) divided by the corresponding increment $\Delta[Cu^{2+}]$ in the copper concentration ($\Delta[Cu^{2+}] = 0.8 \times 10^{-5}$ M).

3.2. EPR measurements

Fig. 5 shows the EPR spectra at 77 K which result from the addition of Cu^{2+} to tRNA. At r values ≤ 0.04 only one Cu^{2+}-tRNA complex (complex I) is visible (fig. 5A). This pattern arises from a paramagnetic Cu^{2+}-tRNA complex displaying an axial symmetry which can be interpreted in term of the following spin Hamiltonian [16]:

$$H = \beta\left[g_{\parallel} H_z S_z + g_{\perp}\left(H_x S_x + H_y S_y\right)\right] + A_{\parallel} S_z I_z + A_{\perp}\left(S_x I_x + S_y I_y\right) \quad (3)$$

where β is the Bohr magneton $g_{\parallel}$ and $A_{\parallel}$ the g value and hyperfine components parallel to the molecular symmetry axis, $g_{\perp}$ and $A_{\perp}$ the g value and hyperfine components perpendicular to the molecular symmetry axis, respectively, S the electron spin ($S = 1/2$) and I the copper nuclear spin ($I = 3/2$).

From the spectrum shown in fig. 5A the following parameters can be measured: $g_{\parallel} = 2.277$, $A_{\parallel} = 140$ G and $g_{\perp} = 2.057$ while $A_{\perp}$ cannot be measured directly. By using the standard formula

$$\mu = \tfrac{1}{3}\left(g_{\parallel} + 2g_{\perp}\right)\left[S(S+1)\right]^{1/2} \quad (4)$$

and inserting the g values measured from the experimental spectrum, the magnetic moment μ can be calculated as 1.85 (in Bohr magnetons, BM), which is in the range expected (1.75–2.20 BM) [17] for simple copper Cu^{2+} complexes lacking Cu-Cu interactions. For EPR spectra indicating a tetragonal environment about Cu^{2+} as in this case, the ratio $g_{\parallel}/A_{\parallel}$ appears to be an empirical index of tetragonal distortion of the equatorial ligands, values ranging from 105 to 135 cm for tetragonal structures and above this for out-of plane distortions toward tetrahedral symmetry [18]. The $g_{\parallel}/A_{\parallel}$ of 147 cm for the Cu^{2+}-tRNA complex of fig. 5A indicates that a slight tetrahedral distortion is present.

As r is increased, another Cu^{2+}-tRNA complex (II) can be observed in addition to the previous one (fig. 5B–E) and at $r = 0.28$ this second complex is prevalent (Fig. 5E). The EPR spectrum of this second complex is superposed on the first one, so it is then quite difficult to determine experimentally the EPR parameters of this new complex. We therefore used a Monte Carlo simulation method

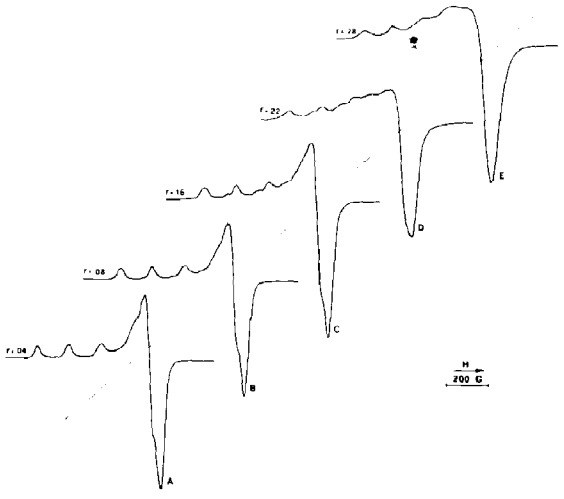

Fig. 5. EPR spectra of Cu^{2+}-tRNA complexes recorded at 77 K at different r values. Microwave power level, 20 mW; magnetic field sweep rate, 2000 G in 8 min; time constant, 0.5 s; modulation amplitude, 5 G.

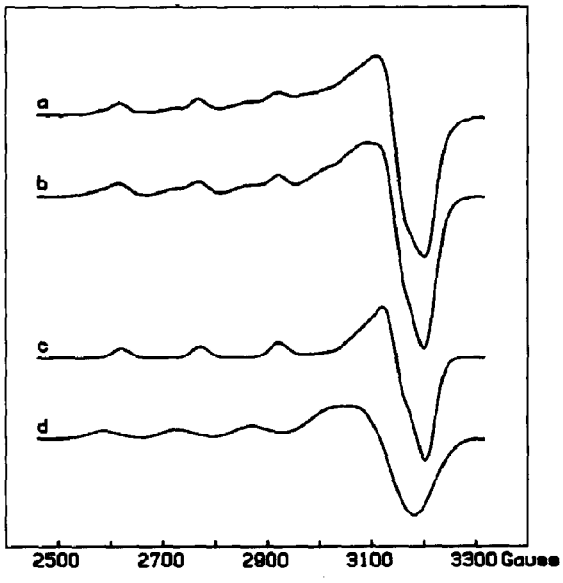

Fig. 6. Experimental (a) and computer-synthesized (b) EPR spectra of Cu^{2+}-tRNA complex. Experimental spectrum, at $r = 0.11$, was recorded as in fig. 5. Spectrum b was the sum of two components due to complex I (c) and complex II (d). Their EPR parameters are reported in table 1.

Table 1

EPR parameters of the Cu^{2+}-tRNA complexes (I and II) as extracted by computer simulation

Parameter	Type I	Type II
$g_z = g_{\|}$	2.277	2.316
$g_x = g_y = g_{\perp}$	2.057	2.069
$A_z = A_{\|}$	140.0	151.0
$A_x = A_y = A_{\perp}$	6.0	16.3
$\Delta H_z = \Delta H_{\|}$	32.7	57.9
$\Delta H_x = \Delta H_y = \Delta H_{\perp}$	41.0	81.4

[19] to obtain a best fit of the experimentally spectra and thence to extract the spin Hamiltonian parameters. The results are shown in fig. 6. The experimental EPR spectrum at $r = 0.11$ is shown in fig. 6a while the computer-simulated spectrum is shown in fig. 6b. The latter spectrum is constituted by the sum of the two spectra reported in fig. 6c and d. As can be observed, the spectrum of fig. 6c bears a very close resemblance to the spectrum related to complex I (at very low r values). The simulation method allowed us to determine all the EPR parameters, even those which could not be measured for complex I. Table 1 summarizes these values. Complex I fitted the Peisach-Blumberg [20] plots for a Cu3N1O or as well for a Cu4N donor set; it is thus quite difficult, on this basis, to assess which ligands the tRNA molecule provides to Cu^{2+}. A measure of the metal-ligand covalency (α^2) can be obtained by using the approximate expression:

$$\alpha^2 = \frac{A_{\|}}{0.036} + (g_{\|} - 2.0023) + \tfrac{3}{7}(g_{\perp} - 2.0023) + 0.04 \qquad (5)$$

(where $A_{\|}$ is in cm^{-1}) which can give an indication of the bonding characteristics of the ligands [21]. The smaller the value of α^2, the greater the covalent nature of the bonding. The α^2 value for the Cu^{2+}-tRNA complex I is 0.76, indicating that the average ligand field provided by tRNA is moderately ionic.

As regards complex II, the $g_{\|}$ and $A_{\|}$ values fitted the Peisach-Blumberg plots for a Cu2N2O donor set. It should be noted that the formation of this second complex is shifted to higher values of r when the ionic strength is increasing (not shown). It is therefore quite probable that phosphate groups are involved in the formation of this second complex.

The $g_{\|}/A_{\|}$ ratio in this case is 157 cm, indicating that a higher tetrahedral distortion is present in this complex as compared with the previous one. Moreover, the calculated α^2 value of 0.78 indicated that in this case, too, the average ligand field is moderately ionic.

4. Conclusions

The present optical and EPR results permit us to draw the following conclusions about the interaction of Cu^{2+} with tRNA molecules. Two distinct paramagnetic Cu^{2+}-tRNA complexes are found: the first, complex I, is observed immediately at very low r values and displays a tetragonal symmetry around the Cu^{2+}, 3 or 4 tRNA nitrogen ligands probably being involved; the second, complex II, becomes detectable at a value of $r = 0.08$ and is the predominant complex at high r values. The formation of this second complex appears to be partly inhibited by the ionic strength. This fact may be indicative of the possible involvement of the tRNA phosphate group in the formation of this complex. On the other hand, the $g_{\|}$ and $A_{\|}$ values of complex II may be consistent with a mixed, oxygen-nitrogen, coordination.

Acknowledgments

This work has been partly supported by a CNR and MPI grant.

References

1 P.R. Schimmel and A.G. Redfield, Annu. Rev. Biophys. Bioeng. 9 (1980) 181.
2 M. Yarus and S. Rashbaum, Biochemistry 11 (1972) 2043.
3 P.E. Cole, S.K. Yang and D.M. Crothers, Biochemistry 11 (1972) 4358.
4 M. Guéron and J.L. Leroy in: ESR and NMR of paramagnetic species in biological and related systems, eds. I. Bertini and R.S. Drago (Reidel, Dordrecht, 1979) p. 327.

5 J.A.L.I. Walters, H.A.M. Geerdes and C.W. Hilbers, Biophys. Chem. 7 (1977) 147.
6 B.R. Reid and G.T. Robilard, Nature (1976) 257–287.
7 A. Stein and D.M. Crothers, Biochemistry 15 (1976) 157.
8 M. Bina-Stein and A. Stein, Biochemistry 15 (1976) 3912.
9 M. Guéron and J. Leroy, Biophys. J 38 (1982) 231.
10 F. Mazzei and G. Onori, Biopolymers 23 (1984) 759.
11 A.S. Brill, R.B. Martin and R.J.P. Williams, in: Electronic aspects of biochemistry ed. B. Pullman (Academic Press, New York, 1964) p. 519.
12 R. Bittman, J. Mol. Biol. 46 (1969) 251.
13 G. Onori and D. Blidaru-Salandi, Inorg. Chim. Acta 80 (1983) 197.
14 J. Bjerrum, C.L. Ballhausen and C.K. Jørgensen, Acta Chem. Scand. 8 (1954) 1275.
15 J.P. Schreiber and M. Daune Biopolymers 8 (1969) 139.
16 B.R. McGarvey, in: Transition metal chemistry, ed. R.L. Carlin (M. Dekker, New York, 1966) p. 89.
17 F.A. Cotton and G. Wilkinson, Advanced inorganic chemistry (John Wiley, New York, 1980).
18 U. Sakaguchi and A.W. Addison, J. Chem. Soc. Dalton Trans. (1979) 600.
19 G. Giugliarelli and S. Cannistraro, Nuovo Cimento 4D (1984) 194.
20 J. Peisach and W.E. Blumberg, Arch. Biochem. Biophys. 165 (1974) 691.
21 D. Kivelson and R. Neiman, J. Chem. Phys. 35 (1961) 149.